


RESEARCH ARTICLE

Changes in atmospheric latent energy transport into the Arctic: Planetary versus synoptic scales

J. H. Rydsaa¹  | R. G. Graversen^{1,2} | T. I. H. Heiskanen¹  | P. J. Stoll¹ 

¹Department of Physics and Technology,
UiT The Arctic University of Norway,
Tromsø, Norway

²Norwegian Meteorological Institute,
Tromsø, Norway

Correspondence

J. H. Rydsaa, Department of Physics and
Technology, UiT The Arctic University of
Norway, Tromsø 9037, Norway.
Email: johanne.h.rydsaa@uit.no

Funding information

Norges Forskningsråd, Grant/Award
Number: 280727; NOTUR Projects,
NN3948k, NS9063k

Abstract

Atmospheric meridional energy transport into the Arctic plays an important role in Arctic weather and climate. The transport of latent energy in the form of water vapour strongly influences the Arctic atmosphere. The transport is achieved by circulation mechanisms on various scales and is largely comprised of extreme transport events. Here, we use a Fourier-based method of dividing the latent energy transport into spatial scales and investigate the extent to which extreme events in latent energy transport on planetary and synoptic scales have changed over the past four decades, and how they influence the Arctic winter temperatures. We find that wintertime extreme transport events on planetary scales are associated with warm temperature anomalies across the entire Arctic, while the extreme events on synoptic scales have less impact on the Arctic temperatures. We show that over the past four decades, there has been a significant increase in the wintertime latent energy transport by planetary-scale systems, and a decrease in synoptic-scale transport. This shift may have contributed to the amplified warming observed in the Arctic winter over the past decades.

KEYWORDS

Arctic amplification, Arctic climate, atmospheric circulation, energy transport, Fourier decomposition, planetary waves, wavelet decomposition

1 | INTRODUCTION

The Arctic has warmed at a rate more than twice the global average over the past decades (Serreze and Francis, 2006; Serreze and Barry, 2011), and this Arctic amplification is strongest during the winter season (Bekryaev *et al.*, 2010; Boisvert and Stroeve, 2015). In recent years, the contribution by atmospheric energy transport to Arctic amplification has received increased attention. Energy transport into the Arctic has been shown to greatly alter the Arctic temperatures (Graversen *et al.*, 2008), and plays an important role in the development of Arctic weather and climate

(Graversen and Burtu, 2016; Woods and Caballero, 2016; Ding *et al.*, 2017; Graham *et al.*, 2017a).

The atmospheric transport of energy is commonly divided into dry static energy (DE) and latent energy (LE) parts, where the latter is associated with a flux of water vapour. The transport of LE has been shown to have a stronger effect on near-surface temperatures as compared to that of DE (Koenigk *et al.*, 2013; Graversen and Burtu, 2016). In addition to the LE that is released upon condensation, the water vapour in itself and the condensed cloud water act to increase the local greenhouse effect and thus the long-wave radiation downwards, hereby

heating the surface (e.g. Graversen and Burtu, 2016; Gong *et al.*, 2017).

Estimates of future energy transport into the Arctic region indicate that in response to climate change, the transport of LE will increase at the expense of that of DE during the twenty-first century, while the total energy transport remains largely unchanged (Hwang *et al.*, 2011; Bengtsson *et al.*, 2013; Koenigk *et al.*, 2013; Skific and Francis, 2013). It has been suggested that this shift from DE towards LE may result in an increased warming in the Arctic region, due to the larger warming effect of LE transport as compared to that of DE (Graversen and Burtu, 2016; Yoshimori *et al.*, 2017; Graversen and Langen, 2019).

Observations show that the Arctic atmosphere has already become warmer and wetter over the past few decades; observed positive trends of clouds and humidity have been explained by a combination of enhanced evaporation from larger ice-free areas inside the Arctic, and convergence of atmospheric LE transported from lower latitudes (Boisvert and Stroeve, 2015). An examination of seven different reanalysis datasets indicates that the main source of atmospheric moisture (~89–94% at 70°N) in the Arctic is provided by transient eddies, typically entering the Arctic via the storm tracks through the northern North Atlantic, Labrador Sea and subpolar North Pacific (Dufour *et al.*, 2016). In the North Atlantic region, advection of moist, warm air from lower latitudes has contributed to as much as a quarter of the observed winter temperature increase in the past couple of decades (Dahlke and Maturilli, 2017), and nearly half of the winter sea ice decline over the period 1979–2011 (Park *et al.*, 2015). Several studies have focused on the occurrence and effects of intense and extreme weather systems that reach far north into the Arctic (e.g. Woods *et al.*, 2013; Liu and Barnes, 2015). Such extreme events are most often the result of a combination of large-scale circulation mechanisms, and favourable local conditions (Simmonds *et al.*, 2008). To investigate the energy transport caused by the different processes contributing to extreme moisture transport into the Arctic, a decomposition of the total energy transport with respect to spatial scale is useful. Studies have shown that energy transport by systems of different scales impact the Arctic differently, and may respond differently to climate change (Graversen and Burtu, 2016; Yoshimori *et al.*, 2017).

Recently, a method of separating the meridional energy transport using a Fourier decomposition into planetary- and synoptic-scale waves was suggested by Graversen and Burtu (2016). The Fourier method differs from the traditional decomposition method as described by Peixoto and Oort (1992) in that it does not separate the transport into transient and stationary parts. In the Fourier

decomposition, waves on all scales can be transient or stationary, and the separation between waves on planetary and synoptic scales is based on their zonal wavelength. By applying this method to the ERA-Interim reanalysis and investigating the energy transport entering the Arctic at 70°N, Graversen and Burtu (2016) found that the LE part of the meridional energy transported on large, planetary scales causes a stronger and more long-lasting impact on near-surface temperatures in the Arctic region than does energy transported on smaller, synoptic scales. Based on this, they suggest that trends in the different scales of the energy transport can cause changes in the Arctic climate, even while the total transport remains the same.

The Fourier decomposition method was evaluated in Heiskanen *et al.* (2020). They found that as it is based on sinusoidal, non-localized functions, it may not fully capture highly localized transport events, which may in some cases lead to an under-representation of the synoptic-scale transport. In comparison to an alternative decomposition method based on wavelets, Heiskanen *et al.* (2020) found that while the Fourier decomposition method occasionally overestimates the planetary-scale transport at the expense of transport on synoptic scales, the wavelet decomposition method underestimates the planetary-scale transport. They conclude that the true estimate of planetary and synoptic transport is between those provided by the two methods. However, they confirm the dominant role of planetary-scale transport in moisture transport into the Arctic.

In addition to being dependent on scales, the impact of LE transport is also dependent on season. Studies have shown that atmospheric energy transport has a large effect on the Arctic winter atmosphere (e.g. Park *et al.*, 2015). Here, we focus on the winter season LE transport, and investigate how the transports on planetary and synoptic scales impact the Arctic winter temperatures. Investigations have primarily been conducted using the Fourier decomposition method. However, to ensure robust conclusions with respect to the representation of systems on both scales, analyses have also been conducted using the wavelet decomposition method.

Given the increases in atmospheric moisture fluxes observed in the Arctic, we further examine whether there have been changes in the separate scales of the energy transport over the past four decades. A large proportion of the LE transport has been shown to be accounted for by a few extreme events each season (Woods *et al.*, 2013). Here we focus on the extreme events on planetary and synoptic scales separately, and show that there have been significant changes in the wintertime LE transport that may have contributed to the amplified warming observed in the Arctic over the past decades.

2 | METHODS AND DATA

The focus of our investigation is on the latent energy transport, as it has been shown to have the strongest effect on Arctic temperatures. The 70°N latitude defines the Arctic border in this study. As the effects of an LE flux entering the Arctic have been shown to vary between seasons, we focus our investigations on impacts and trends on the wintertime transport.

We use the recently released ERA5 dataset (Hersbach *et al.*, 2020), which is a state-of-the-art reanalysis with a resolution 0.25°. Due to a mass-flux inconsistency in reanalysis data (Trenberth, 1991), a barotropic mass-flux correction has been applied to the wind field at each time step (Graversen, 2006).

We now separate the latent energy into planetary-scale transport and synoptic-scale transport, following the newly developed Fourier-based approach presented by Graversen and Burtu (2016) and evaluated by Heiskanen *et al.* (2020). The meridional latent energy transport can be expressed as

$$\overline{vQ}(\phi) = \oint \int_0^{p_s} vLq \frac{dp}{g} dx, \quad (1)$$

where ϕ is latitude, $\mathbf{v} = (u, v)$ is the zonal and meridional wind components, x is the coordinate in the eastward direction, L the latent heat of condensation, q the specific humidity, p the atmospheric pressure, and g is the gravitational acceleration. By employing a Fourier transformation of the mass flux $v \frac{dp}{g}$ and Lq , one can obtain a decomposition of the latent energy transport planetary- and synoptic-scale waves. For Lq , the transformation yields

$$Lq = \frac{a_0^L}{2} + \sum_{n=1}^{\infty} \left\{ a_n^L \cos\left(\frac{n 2\pi x}{d}\right) + b_n^L \sin\left(\frac{n 2\pi x}{d}\right) \right\}, \quad (2)$$

where

$$a_n^L = \frac{2}{d} \oint Lq \cos\left(\frac{n 2\pi x}{d}\right) dx \quad (3)$$

and

$$b_n^L = \frac{2}{d} \oint Lq \sin\left(\frac{n 2\pi x}{d}\right) dx, \quad (4)$$

where a_n^L and b_n^L are functions of latitude, height and time, and $d = 2\pi R \cos(\phi)$, where R is the Earth's radius. Corresponding coefficients are obtained for $v \frac{dp}{g}$, and by applying the Fourier series of the mass flux and Lq into Equation (1), the meridional transport can be decomposed into wave parts which are defined as representing planetary or synoptic scales. Here, we choose a slightly different definition of planetary and synoptic scales to what was used in Graversen and Burtu (2016): based on the findings in the

evaluating study by Heiskanen *et al.* (2020), we apply a division between planetary and synoptic scales between wave numbers 3 ($\sim 4,500$ km at 70°N) and 4 ($\sim 3,400$ km at 70°N). This yields a planetary-scale transport comprised of waves greater than $\sim 4,000$ km at 70°, which is a good approximation of actual planetary length-scales at 70°N according to Holton and Hakim (2013). The latent transport associated with planetary- and synoptic-scale waves can then be expressed as

$$\overline{vQ_P} = d \sum_{n=1}^3 \left\{ \sum_{k=1}^K \frac{1}{2} (a_n^v a_n^L + b_n^v b_n^L) \right\} \quad (5)$$

and

$$\overline{vQ_S} = d \sum_{n \geq 4} \left\{ \sum_{k=1}^K \frac{1}{2} (a_n^v a_n^L + b_n^v b_n^L) \right\}, \quad (6)$$

respectively, where overbar indicates zonal integrals and index k represents all model hybrid levels from 1 to K . Hence $\overline{vQ_P}$ and $\overline{vQ_S}$ are functions of latitude and time only. By applying the Fourier decomposition on the mass flux, transports as function of longitude in addition to latitude and time can be obtained by

$$vQ_P = \sum_{n=1}^3 \left\{ \sum_{k=1}^K \left(a_n^v \cos\left(\frac{n 2\pi x}{d}\right) + b_n^v \sin\left(\frac{n 2\pi x}{d}\right) \right) Lq \right\}, \quad (7)$$

and

$$vQ_S = \sum_{n \geq 4} \left\{ \sum_{k=1}^K \left(a_n^v \cos\left(\frac{n 2\pi x}{d}\right) + b_n^v \sin\left(\frac{n 2\pi x}{d}\right) \right) Lq \right\}, \quad (8)$$

respectively. This longitudinal-dependent decomposition could also have been based on a Fourier decomposition of the Lq field rather than the mass flux. However, the mass flux is closely related to the structure of the geopotential height field from which Rossby waves, cyclones and other wave structures are normally revealed. Note that zonal integrals of this longitudinal decomposition of the transport are equal to the components $\overline{vQ_P}$ and $\overline{vQ_S}$ as defined above.

An alternative decomposition method based on wavelets was proposed in Heiskanen *et al.* (2020). The wavelet decomposition method is based on a set of localized functions known as wavelets, and similar to the Fourier method, these functions decompose the energy transport into parts with different length-scales. Hence the method can also be used to decompose the latent energy transport into planetary and synoptic scales. As it is based on localized functions, the method is expected to better represent highly localized synoptic-scale systems. Here, all analyses have also been conducted using the wavelets

method, which is applied to the ERA-Interim dataset. The results from this analysis are largely similar to the Fourier decomposition, and the main conclusions drawn remain the same. More detail of the wavelet decomposition method, along with results of the associated analysis are found in Appendix S1.

The investigations presented here are focused on the latent energy transport and its effects on Arctic temperatures. Several studies have shown that a disproportionately large amount of atmospheric moisture is transported into the Arctic region by the most extreme transport events (e.g. Woods *et al.*, 2013; Liu and Barnes, 2015). Similar to those studies, we focus on the most extreme transport events, which are defined here as days where the zonal-mean transport anomaly at 70°N exceeds the 90th percentile as computed per season on planetary and synoptic scales. Anomalies are deviations from the smoothed seasonal mean, based on the full 40-year time series.

To understand the effect of extreme transport events on Arctic temperatures, we investigate the typical patterns of temperature anomalies arising around the time of such events in the form of composite plots. The composites are computed as averages of the daily-mean locally de-seasonalized temperature anomalies. The temperature anomalies are de-trended locally using a 4th-degree polynomial fit. Statistically significant areas are identified by a Monte Carlo approach; the selection of days is compared to 5,000 random selections of days from the same season, and only the areas that have a larger absolute value of anomalies in less than 5% of the cases are considered significant at the 95% level. For days identified as extreme, the location of the peak of LE transport along 70°N is identified from the longitude-dependent decomposition, which aids in linking the trends identified here to large-scale circulation changes.

3 | RESULTS

3.1 | Locations of extreme events

Figure 1 shows the longitudinal distribution of winter season LE transport across 70°N on days identified as extreme. Each curve shows the daily mean latent energy transport anomaly as a function of longitude on days that exceed the seasonal 90th percentile on the planetary scale (upper panel) and the synoptic scale (lower panel). Areas with highly (weakly) saturated colour indicate several (few) superimposed curves, that is, common (uncommon) longitudes of transport on extreme days. Most curves are dominated by one distinct peak, which indicates one main transport event on the extreme day that

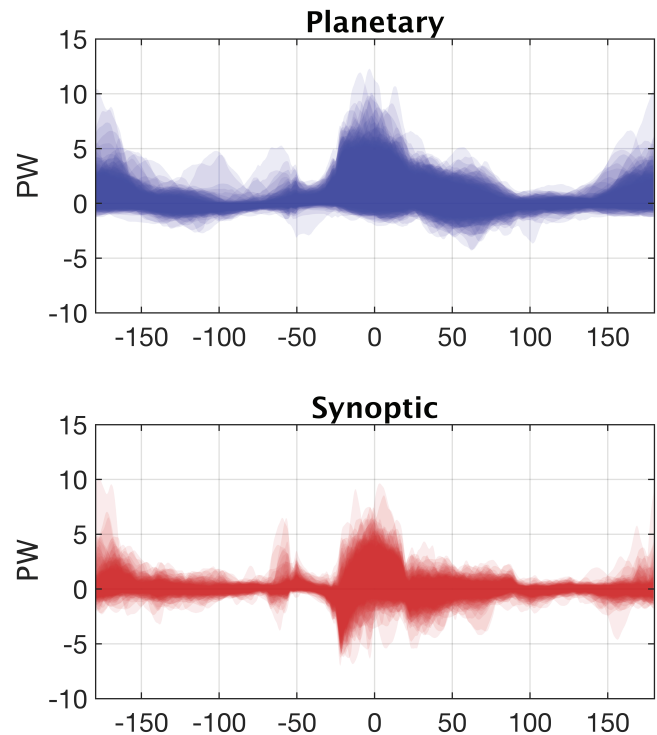


FIGURE 1 Extreme latent transport (PW) as a function of longitude (°E) along 70°N for all winter season extreme cases as curves with transparent shading superimposed on top of each other. Each curve represents the latent energy transport anomalies across 70°N for a day above the 90th percentile level. More saturated colour indicates overlapping curves, i.e. areas with high frequency of transport on extreme days; planetary scale is shown in the upper panel, and synoptic scale in the lower panel

curve represents. In most cases the peaks, that is, the locations of the extreme events, are concentrated above the relatively warm open ocean areas, namely the Atlantic sector and the Bering Strait, on both scales. A similar pattern of extreme transport events being concentrated over the warm ocean basins in winter has also been observed in other studies (Woods *et al.*, 2013; Liu and Barnes, 2015; Woods and Caballero, 2016).

On the synoptic scale the latent energy transport is associated with, for example, cyclones entering the Arctic and bringing water vapour with them. Particularly in the Atlantic sector, the northward component of the cyclonic circulation is clearly shown as positive peaks at the eastern side of the cyclones, and the southward component seen as a sharp negative peak on the western side of it (Figure 1, lower panel).

In general, the planetary-scale events bring more latent energy to the Arctic. Overall, the wintertime latent energy transport on the synoptic and planetary scales accounts for 32% and 68% of the total wintertime transport, respectively (based on the sum of daily means). The extreme winter days on the planetary scale account for 33% of the total

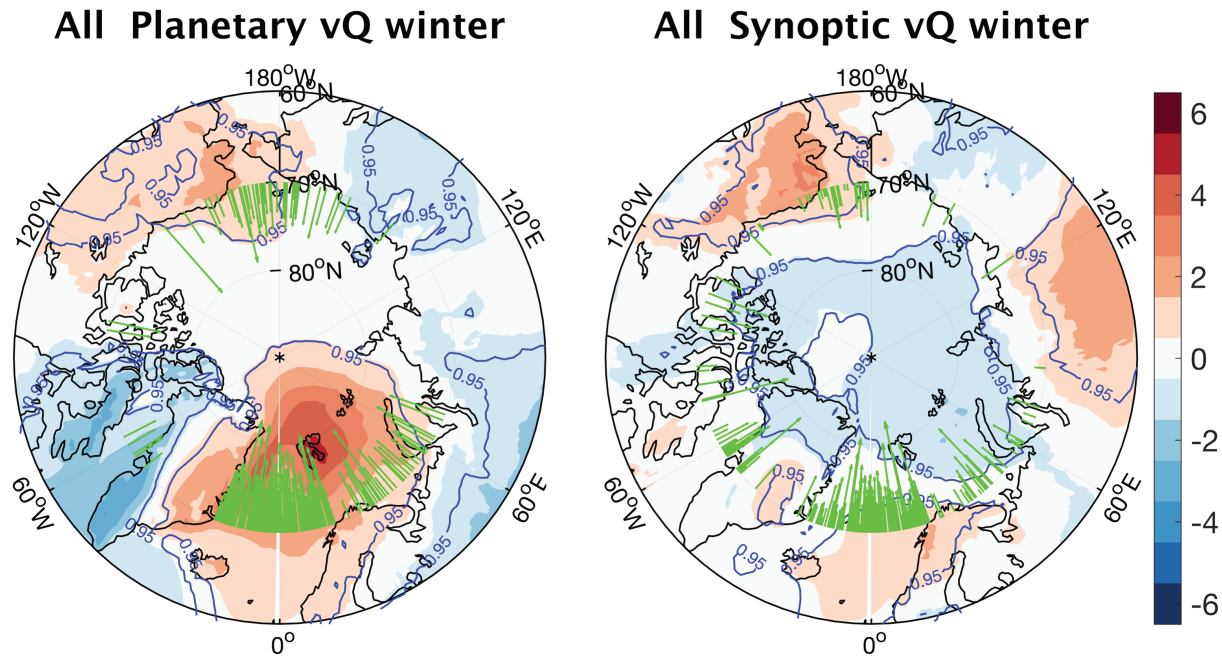


FIGURE 2 Mean temperature anomalies ($^{\circ}\text{C}$) related to extreme (>90 th percentile) latent energy transport anomalies across 70°N . Green arrows along 70°N indicate the point of maximum transport anomaly for each extreme day. The length of the arrows is scaled to one-degree latitude per PW latent energy, and as such does not reflect the extent to which the transport reaches into the Arctic area. Blue lines enclose areas with statistically significant results according to a Monte Carlo test for significance with 5,000 simulations

planetary transport, and about 22% of the total transport. The synoptic-scale extreme days account for about 34% of the total synoptic transport, and 11% of the total transport.

The temperature pattern associated with extreme transport events is shown as temperature anomalies as averaged over extreme transport days on both length-scales (Figure 2). An arrow marking the location of the peak transport anomaly each day is added along the 70°N latitude. Note that the arrows are scaled according to the strength of the event and are not indicative of how far into the Arctic the transport reaches.

There are significant temperature anomalies inside the Arctic associated with extreme events on both synoptic and planetary scales; however, they are of opposite signs: planetary-scale events are associated with warm anomalies inside the Arctic (Figure 2, left panel), while synoptic-scale events are associated with cold anomalies (Figure 2, right panel). During planetary-scale extreme events, the warm temperature anomalies are concentrated around the areas where the peak transport most often occurs, and the largest warm anomaly is centred over the Svalbard region and stretches as far as the North Pole. The average temperature anomaly for the Arctic as a whole during planetary events is $+0.63\text{ K}$. The Atlantic sector (defined here as -40° to $+60^{\circ}\text{E}$), contributes with 77% of the wintertime planetary events, and therefore dominates the mean temperature pattern. Accounting only for the

events and temperature anomalies occurring within these longitudes, the average temperature increase in the sector is 2.67 K .

On days with strong synoptic transport (Figure 2, right panel), the Arctic region is on average dominated by anomalously cold temperatures (-0.37 K), while warm areas are found just outside and to the south of the extreme transport events. The temperature patterns seem to be closely associated with an atmospheric situation favourable for synoptic-scale events; a sharp temperature gradient across 70°N with cold air to the north and warm anomalies to the south can act to increase baroclinicity necessary for creating an extreme synoptic event. This temperature profile is similar to findings in Graversen and Burtu (2016), who by performing a regression analysis of near-surface temperatures on synoptic-scale energy transport, found a similar pattern in the zonal average.

The large differences in the mean temperature patterns associated with the two scales reflect the different circulation types responsible for the energy transport on each scale. The fact that the impact of these circulation types are so clearly revealed in the temperature composites suggests that the decomposition of the energy transport into different scales is important, and that the division between planetary and synoptic scales as defined here is capable of capturing typical transport situations on each scale. Also, the pattern for mean temperature anomalies shows very

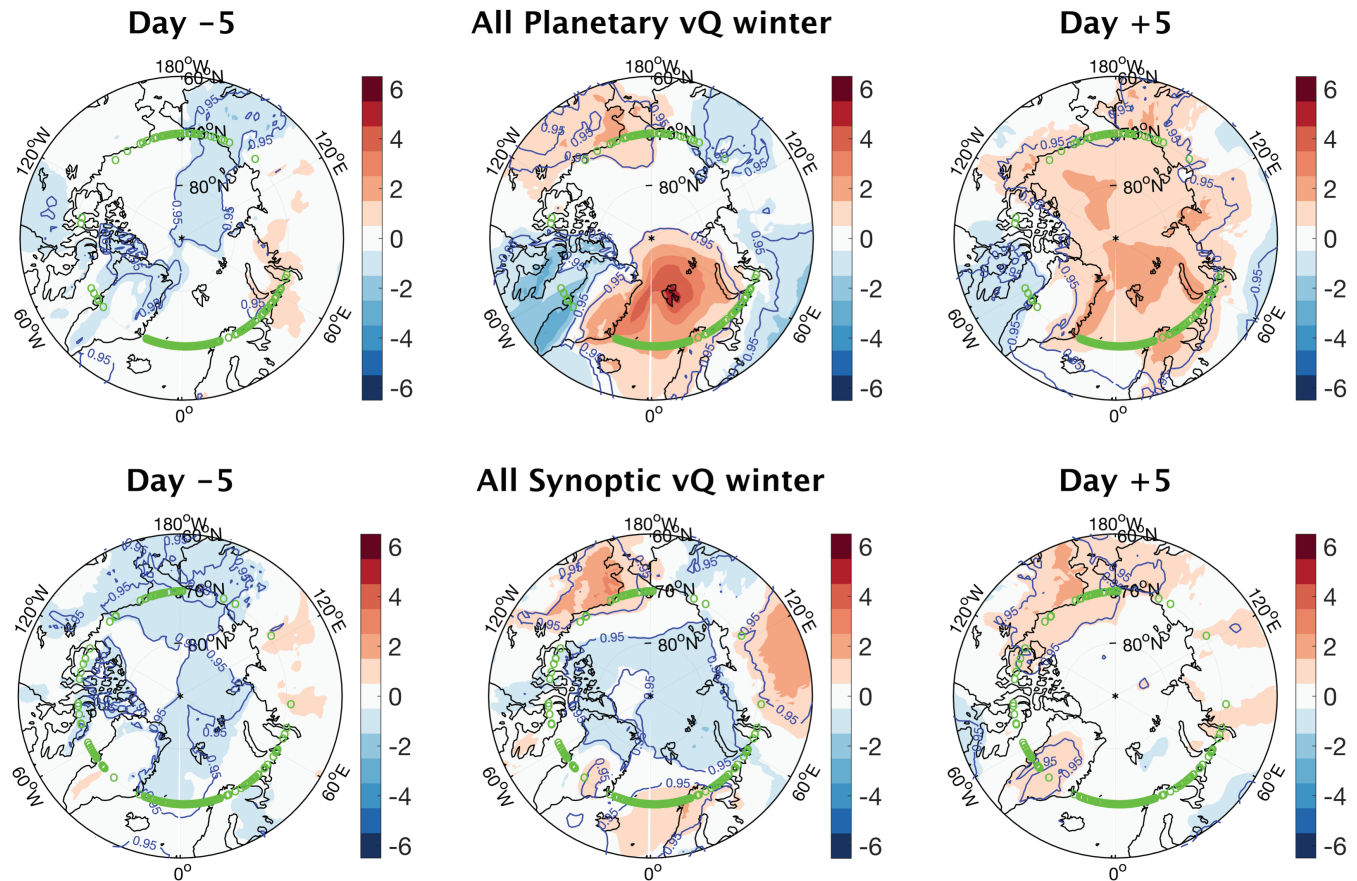


FIGURE 3 Temperature anomalies as averaged over days of extreme transport entering the Arctic (maximum transport locations shown as green dots). Temperature anomalies 5 days ahead of events (left column) on the day of extreme transport events (middle column) and 5 days after events (right column) for planetary-scale events (upper row) and synoptic-scale events (lower row). Blue lines surround areas with statistically significant anomalies

similar results when compared to composites based on the wavelet decomposition method, both with regard to strength and geographical distribution of the temperature anomalies (Figure S1, supplementary material).

The time-development in surface temperature anomalies in response to the extreme events on each wave scale is seen in Figure 3, which shows the mean temperature anomalies before, during and after extreme transport events. On the planetary scale (Figure 3, top row), the warm anomaly appears on the day with extreme transport, and 5 days later it has spread across most of the Arctic basin (Figure 3, top-right panel). Although the largest temperature anomalies are seen locally in the Svalbard region on the day of the extreme transport event, the Arctic area as a whole is most influenced a few days after the planetary-scale event.

On the synoptic scale, anomalously cold temperatures inside the Arctic region before the events and during the events dominate the mean temperature anomaly development (Figure 3, lower row). Five days after the events, the

cold anomalies inside the Arctic region have been broken up, and the anomalous temperature gradient across 70°N is dissolved (Figure 3, lower-right panel), leaving no significant anomalies inside the Arctic region.

It may be inferred from this analysis that the planetary-scale events are closely associated with unusually warm temperatures in the Arctic region, while the synoptic-scale extreme events mainly contribute by dissolving preconditioning temperature gradients with Arctic cold anomalies.

The composite plots show the temperature anomalies associated with extreme events as averaged over several different extreme days; however, they do not show the potential for temperature changes that actually occur during each event, which can be much more dramatic. To illustrate the type of situation that these extreme events represent, we have included a case from the N-ICE2015 measurement campaign (Cohen *et al.*, 2017; Graham *et al.*, 2017b) that took place north of Spitsbergen in January 2015.

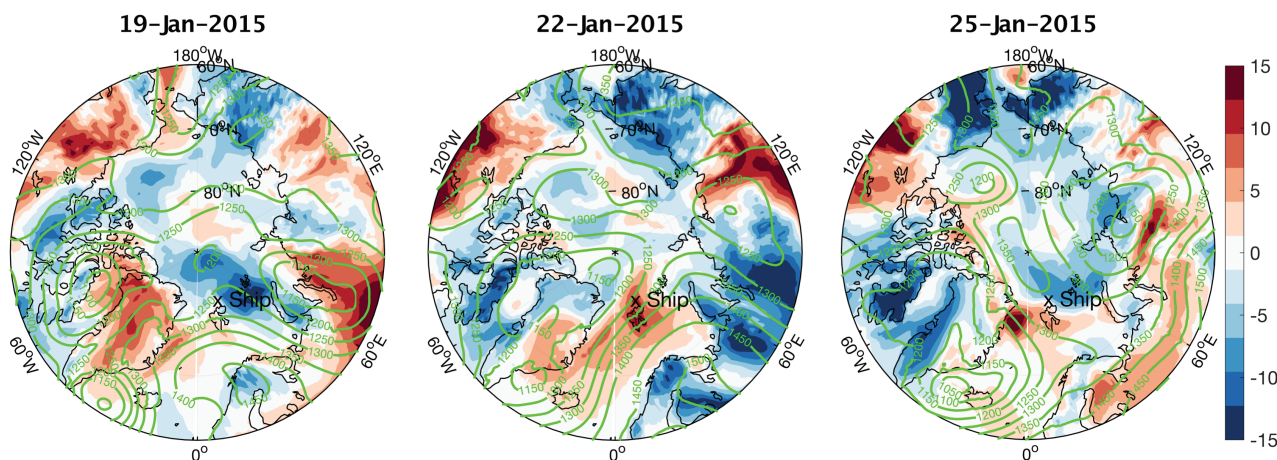


FIGURE 4 Temperature anomalies ($^{\circ}\text{C}$) on 22 January 2015 (middle) and 3 days before (left) and after (right). Green contour lines show the geopotential height at 850 hPa. The ship's approximate position on 22 January is marked north of Svalbard

3.2 | Case: Spitsbergen, 22 January 2015

The Norwegian Young Sea Ice expedition (N-ICE2015) was a ship-based measurement campaign based on in-ice drift in the area north of Svalbard throughout the winter and spring season of 2015. During this campaign, atmospheric measurements of temperature, wind speed and wind direction, air pressure and air humidity were conducted from both the Norwegian Polar Institute's research vessel *Lance* and from measurement towers launched on icefloes.

Based on this campaign, Graham *et al.* (2017b) describe two typical atmospheric states occurring during the winter season; the most common was a “radiatively clear state”, with cold temperatures, mostly clear skies and stable conditions. This was regularly disrupted by storms leading to periods of a “radiative opaque state” with increased cloud cover and atmospheric moisture, and drastic increases in temperature of up to 30 K, from around -30°C to around zero. These storm events would normally last for a few days. Typically, the strong events measured north of Spitsbergen were part of large-scale circulation patterns. Graham *et al.* (2017b) also highlight that the entire winter period of the N-ICE2015 campaign was characterized by an anomalously large meridional component of the jet stream that drove several intense storms into the high Arctic (north of 80°N).

One such episode occurred on 21–22 January 2015. Figure 4 shows the temperature anomalies associated with this event, along with the geopotential height contours at 850 hPa, 3 days ahead of, during, and 3 days after the event. On the day of the event, we see temperature anomalies of up to $+15\text{K}$ centred around the Svalbard region, and geopotential height contours indicate a strong south-westerly geostrophic wind component (Figure 4, middle panel).

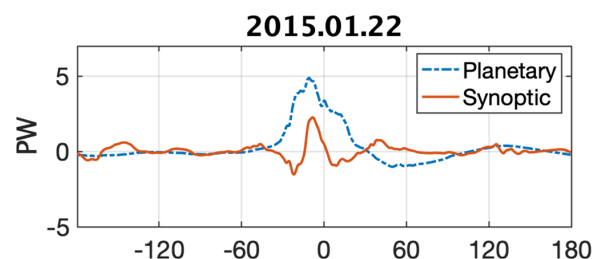


FIGURE 5 Daily mean latent energy transport anomaly (PW) across 70°N on 22 January 2015, as a function of longitude ($^{\circ}\text{E}$). The planetary-scale transport is comprised of waves 1–3, and the synoptic-scale transport of waves 4–21 [Colour figure can be viewed at wileyonlinelibrary.com]

Based on the Fourier decomposition of the transport along 70°N on this particular day (Figure 5), we see that the transport on that day is concentrated just southeast of Spitsbergen, for both the planetary-scale and the synoptic-scale transport. The planetary-scale transport dominates, reflecting the large-scale component of the event.

In the Fourier decomposition, 22 January is recognized as an extreme transport event on the planetary scale, i.e. a day when the planetary-scale transport exceeded the 90th percentile for the 2015 winter season. This corresponds well with the observations of the anomalously large meridional component of the jet stream over this area, as noted by Cohen *et al.* (2017). The energy transport and this particular event is as such described as being a result of atmospheric mechanisms on various scales.

However, one should also note that the synoptic-scale transport is large in this area, even though this anomaly is not large enough to qualify as an extreme case during this season. The local cyclone's contribution to the decomposed transport is captured by the synoptic-scale

TABLE 1 Trends in energy transport components ($\text{PW}\cdot\text{decade}^{-1}$). Trends are based on a linear regression of seasonal averages of daily values

	DJF	MAM	JJA	SON
Planetary vQ	0.005 ($p = .07$)	-0.002 ($p = .23$)	-0.001 ($p = .36$)	0.0008 ($p = .41$)
Synoptic vQ	-0.003 ($p = .03$)	0.002 ($p = .14$)	0.0055 ($p = .04$)	-0.0015 ($p = .23$)

Note: Bold numbers indicate trends that are statistically significant at a 90% level, according to a Monte Carlo type test with 5,000 simulations. Three-monthly, starting in December.

waves, but again it does not impact the zonal average transport enough to qualify the daily mean transport anomaly as an extreme event.

The aim with presenting this case-study is to show an example of how energy transport from a particular and well-documented extreme event is represented by the Fourier decomposition method. It illustrates key features of the Fourier decomposition method; by decomposing the transport of this event into different spatial scales, it is able to identify the large-scale transport as the more unusual part of the total event, even though the synoptic-scale transport also played an important role.

However, as previously mentioned, it is important to keep in mind that a highly localized single event may not be fully represented by the Fourier method if it is that this method relies on sinusoidal waves (Heiskanen *et al.*, 2020). In such cases the method may underestimate the transport from the synoptic-scale part of the transport to some degree. However, applying the wavelets decomposition method as proposed by Heiskanen *et al.* (2020), which better represents highly localized systems, confirms that this is not a synoptic-scale extreme transport event (not shown).

3.3 | Changes in transport components

The LE transport on various scales and seasons affects the Arctic in different ways. Changes in the relative magnitude of planetary- and synoptic-scale transport may therefore have contributed to Arctic climate change. Here, we investigate whether such changes can be identified in the four decades of data covered by the ERA5 dataset.

By using a simple least-squares regression analysis on annual mean anomalies for the 40-year period (1979–2018) we find that the LE transport increased slightly over the past 40 years (not statistically significant). By investigating the trends in mean seasonal anomalies across the 40 years, we find significant trends in both the summer (Table 1) and winter seasons (Figure 6).

We find a mean increase in the winter season LE transport by planetary waves across 70°N of $0.005 \text{ PW}\cdot\text{decade}^{-1}$ (p -value = .07), and the synoptic transport decrease over

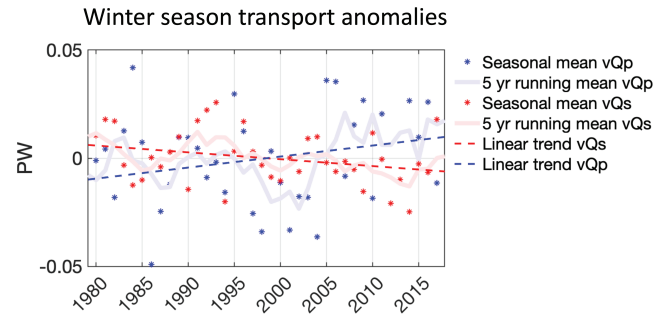


FIGURE 6 Seasonal anomalies in latent energy transport (dots, PW) for planetary-scale transport (blue) and synoptic-scale transport (red), by year. Thick lines show a 5-year moving average, and stippled lines the linear trends based on linear regression. LE transport by planetary waves across 70°N increase $0.005 \text{ PW}\cdot\text{decade}^{-1}$ (p -value = .07). The winter season synoptic transport decreases by $0.003 \text{ PW}\cdot\text{decade}^{-1}$ (p -value = .03). Statistical significance is based on a Monte Carlo approach with 5,000 simulations

the same period by $0.003 \text{ PW}\cdot\text{decade}^{-1}$ (p -value = .03) (Figure 6). Due to the larger temperature effect related to latent energy transport in winter as compared to summer, we focus on the winter season; however, trends for both scales and all seasons are given in Table 1.

3.4 | Changes in the extreme cases

When investigating the upper percentiles of the seasonal trends, we find that the increase in the mean winter-time transport by planetary-scale waves is largely owing to an increase in the uppermost extreme transport events (Figure 7). The increase is larger (as indicated by steeper trend lines) for higher percentile values, indicating that the seasonal level of extreme cases on average increases through the period.

The same pattern is seen in the decrease in transport by synoptic-scale systems, which is also largely owing to a decrease in the upper extreme values (Figure 7, bottom panel). The lower percentiles show no specific trends on either scale (not shown). The explanation for this increase in the level of very strong transport events might

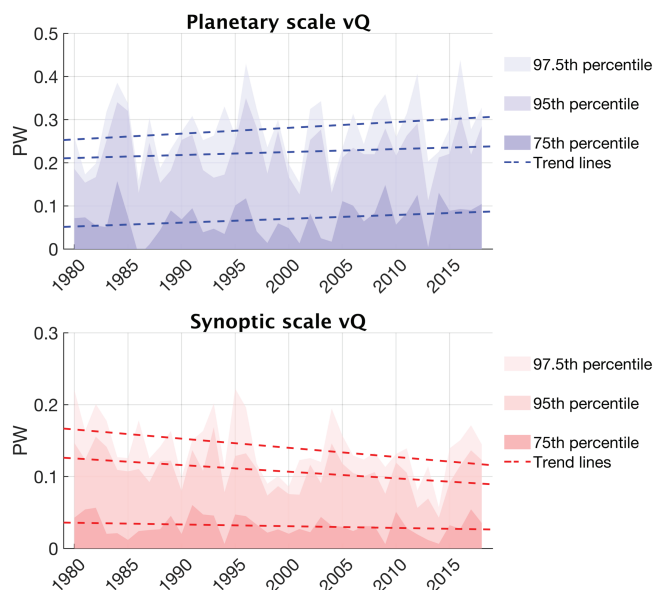


FIGURE 7 Seasonal mean winter (December–February) anomalies in latent energy transport (PW) across 70°N by planetary-scale waves (upper panel) and synoptic-scale waves (lower panel) over the time period 1979–2018. Shading indicates the 75th, 95th and 97.5th percentiles per winter season, from weakly to heavily transparent colours, respectively. Stippled lines indicate the linear trends in the respective percentile values. Note the difference in scale between panels

lie with the general increase in humidity in the atmosphere causing strong transport events to increase, or with circulation changes causing increased winds and transport, or a combination of both. As the former explanation should lead to a general increase of the transport on all levels, this skewed increase might point in the direction of the latter.

The same overall pattern of trends in the wintertime LE transport is found in the ERA-Interim dataset decomposed by the wavelet decomposition method (Figure S2 and S3), which inherently has a negligibly different distribution of planetary- and synoptic-scale events as compared to the Fourier method. This shows that the trends are not sensitive to the method of decomposition, and rather a robust feature of the energy transport.

A decrease in strong cyclones over the past decades is also confirmed in a completely alternative method of identifying synoptic-scale systems. In this method, cyclone track points were identified as in the cyclone tracking algorithm by Hodges (1999). From the 6-hourly ERA-Interim dataset, track points were identified by local maxima exceeding a threshold of $5 \times 10^{-5} \text{ s}^{-1}$ in the relative vorticity spectrally filtered between wave numbers 40 and 100. For the comparison, only cyclone track points within a latitude belt of $70^\circ\text{N} \pm 2^\circ$ were considered. In this dataset we also observe a downward trend in the intensity of the

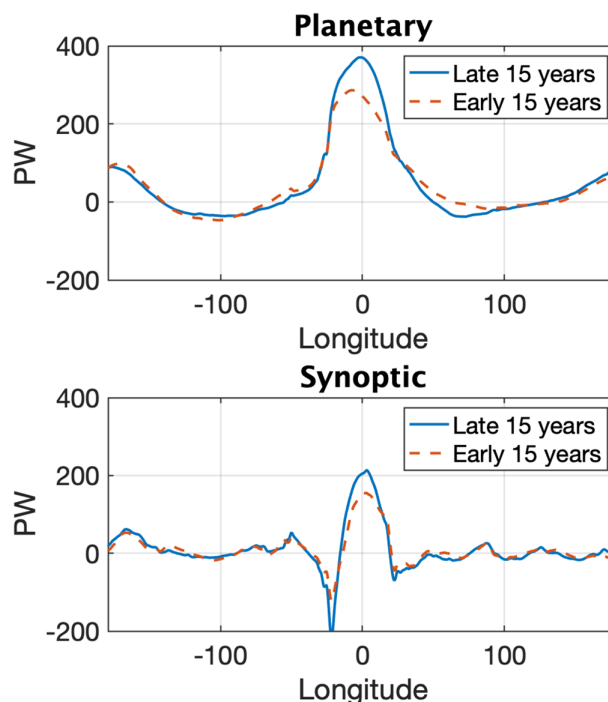


FIGURE 8 Distribution of latent energy transport along 70°N shown as sum of daily mean energy (PW) for days with extreme transport events (exceeding the 90th percentile of each season), by longitude (°E). Stippled lines shows the sum of extreme days over the early 15 winter seasons (1979–1993), while whole lines shows extreme days over the late 15 winter seasons (2004–2018) [Colour figure can be viewed at wileyonlinelibrary.com]

97.5th percentile as computed per season (Figure S4). This is consistent with our findings of a decreasing trend in wintertime strong cyclones passing the 70°N latitude and into the Arctic.

By comparing the first 15 to the last 15 winter seasons of the 40-year time series, we can investigate changes in the placement of extreme transport events. There have been no major shifts in the locations of the planetary- and synoptic-scale systems entering the Arctic region along the 70°N latitude (Figure 8). The main changes are found in the Atlantic sector, where the extreme events in wintertime planetary transport are about 100 PW larger over the last as compared to the early 15 years (Figure 8, top panel). This is consistent with findings showing that this area has experienced an increase in temperatures and downwards longwave radiation (LWD) over recent decades which has been shown to have been driven by an increased atmospheric moisture advection from lower latitudes due to changes in the large-scale atmospheric circulation (Park *et al.*, 2015). On the synoptic scale (Figure 8, lower panel), a smaller increase can be seen in the northward direction, and there is also an increase in the southward direction, west of the northward peak.

4 | DISCUSSION

When we examine the mean LE transport across 70°N over the past 40 years, we find a positive trend in the wintertime LE transport anomalies on the planetary scale, with the steepest increase in the most extreme events. This trend is important as we find that extreme events in wintertime latent energy transport by planetary-scale systems are more closely associated with anomalous warming in the Arctic than extreme transport events by the synoptic-scale systems. The warm anomalies last for several days and spread across the entire Arctic basin. This dependence on wave scale confirms findings by Graversen and Burtu (2016). In our study, a planetary-scale extreme event on average raises the mean temperature by 0.6 K in winter, averaged across the Arctic (>70°N). However, the warming as well as the majority of extreme cases are concentrated in the North Atlantic area where the associated area-average warming during extreme events is 2.6 K in winter. Comparing the early 15 to the latest 15 winter seasons, we see that the changes in extreme transport events are also mainly confined to the North Atlantic region. It is likely that the positive trend in planetary-scale extreme events in this area, combined with the strong warming signal associated with such events, have contributed to the increased warming observed in the North Atlantic Arctic area over the past decades. It is also consistent with findings of increased LE flux into this area over the past decades (Park *et al.*, 2015; Woods and Caballero, 2016; Dahlke and Maturilli, 2017; Graham *et al.*, 2017a). Dahlke and Maturilli (2017) also showed an increase in the duration of strong wintertime warming events in the North Atlantic region of the Arctic of 0.45 K·decade⁻¹ over the past decades, which is coherent with an increase in the planetary-scale events, which on average warm the Arctic over several days.

On the synoptic scale, we find that extreme transport events across 70°N have decreased in winter over the past four decades, and that the decrease is largest for the most extreme events. During synoptic-scale events, cold temperature anomalies dominate as averaged over 5 days before and during the events. Temperature anomalies 5 days after synoptic events are small, and the significant anomalies in the temperature gradients appear to have been dissolved.

For the synoptic scale, it seems that the associated temperature patterns are responsible for the synoptic-scale transport events, rather than the response to them. As the synoptic-scale systems are largely driven by local temperature gradients acting to increase the baroclinicity, increased winter temperatures in the Barents and Kara Seas may have contributed to a decrease in extreme transport events across 70°N in the North Atlantic, where also the majority of extreme synoptic events in winter occur.

The Barents and Kara Seas have been identified as the most prominent area for Arctic amplified warming (Park *et al.*, 2015). This warming has been shown to cause shifts in the synoptic-scale activity in the area due to decreased temperature gradient, and may have caused strong cyclone activity to decrease and/or shift paths (Inoue *et al.*, 2012).

The decrease in synoptic-scale transport across 70°N is also confirmed using the wavelet decomposition method, and with a completely alternative method of identifying synoptic-scale events, based on a cyclone tracking algorithm applied to the ERA-Interim reanalysis. The same pattern of strong decrease in intensity of wintertime extreme events is seen in these datasets, although trends are smaller than in the Fourier-based decomposition.

Synoptic-scale storm systems are often closely related to large, planetary-scale circulation systems (Simmonds *et al.*, 2008) and as such, a typical strong storm in high latitudes is often a result of a combination of large-scale circulation systems and favourable local conditions. The combination is responsible for bringing large amounts of latent energy into the Arctic. For example, large blocking systems can act to deflect small synoptic-scale systems northward, as observed by Woods *et al.* (2013), resulting in these synoptic-scale systems reaching further north and deeper into the Arctic. Cohen *et al.* (2017) similarly observed that strong wintertime storm systems in the Svalbard region were steered north by a large-scale hemispheric circulation pattern. In such cases, where the synoptic system is part of a greater circulation pattern, the associated energy transport may contribute to either scale in the Fourier decomposition. Papritz and Dunn-Sigouin (2020) showed that the planetary-scale transport is closely linked to large-scale blocking situations that act to deflect cyclone tracks poleward, thereby causing a strong northward transport in the interaction between the blocking system and upstream cyclones.

Therefore, our finding of increased planetary-scale transport and other findings of increase in extreme synoptic events (e.g. Rinke *et al.*, 2017) is not conflicting, but rather describes different features of the same trends. This is exemplified in the case-study selected here: In the case-study from the N-ICE2015 measurement campaign, a planetary-scale circulation pattern with a particularly strong northward component of the polar jet stream was identified as necessary for the synoptic-scale storm system to reach the measurements site north of Svalbard, as described by Cohen *et al.* (2017). This event was recognized as an extreme transport event on the planetary scale using the Fourier decomposition method. On the synoptic scale, the storm system as experienced from the ship was not recognized as particularly extreme.

This is further exemplified in Heiskanen *et al.* (2020), who evaluated the Fourier method for estimating

planetary- and synoptic-scale transport, and compared it to an alternative method using wavelets. The alternative wavelet method, which is based on localized functions, proved more skilful at resolving synoptic-scale single systems. With regard to the case studied here, the wavelet method confirmed that the event did not qualify as an extreme event on the synoptic scale. However, the wavelet method did not confirm that planetary-scale transport was an extreme event as proposed by the Fourier method, but this could be related to the wavelet method's risk of under-representing planetary-scale events.

In Heiskanen *et al.* (2020), regression analyses using both methods show a strong warming signal inside the Arctic resulting from planetary-scale transport, and a much weaker signal associated with synoptic-scale transport; however, the distribution is more even in the wavelet method as compared to the Fourier method. Here, we have chosen to lower the wave number of the split between planetary and synoptic scales as compared to that in Graversen and Burtu (2016), as suggested in Heiskanen *et al.* (2020), to better represent the wavelengths of planetary- and synoptic-scale systems in high latitudes. By performing the same type of analysis of the extreme events on each scale while using the wavelet decomposition method, we find that the same wintertime trends and general pattern of temperature anomalies associated with extreme events as in the Fourier decomposition dataset. This shows that the conclusions drawn here are not sensitive to the decomposition method, but rather robust features of synoptic- and planetary-scale energy transport.

5 | CONCLUDING REMARKS


We find a mean decrease in wintertime synoptic-scale transport and an increase in planetary-scale transport over the past 40 years. We show that this shift has the potential to both increase the amount of latent energy that reaches deep into the high Arctic, and to contribute to increased winter season warming, even if the total annual mean energy transport stays the same. The effect of LE transport on Arctic climate has been documented thoroughly; however, to our knowledge, this is the first study to quantify the seasonal trends of the planetary- and synoptic-scale components of the transient meridional energy transport separately. These findings contribute to explaining the increase in LE fluxes and warm winter periods observed in the Arctic over the past decades. Lastly, these results raise questions about mechanisms responsible for the identified trends in planetary- and synoptic-scale LE transport in winter, and to future impact of these changes on the Arctic climate.

ACKNOWLEDGEMENTS

This work was funded by the Norwegian Research Council (NFR) under the project “The role of the atmospheric energy transport in recent Arctic climate change” (project no. 280727), and the NOTUR projects NN3948k and NS9063k. We would like to thank the ERA5 group and the ERA-Interim team for providing the datasets for these analyses.

ORCID

J. H. Rydsaa  <https://orcid.org/0000-0002-0538-0714>

T. I. H. Heiskanen  <https://orcid.org/0000-0003-0113-0627>

P. J. Stoll  <https://orcid.org/0000-0003-1120-2049>

REFERENCES

- Bekryaev, R.V., Polyakov, I.V. and Alexeev, V.A. (2010) Role of polar amplification in long-term surface air temperature variations and modern Arctic warming. *Journal of Climate*, 23, 3888–3906.
- Bengtsson, L., Hodges, K.I., Koumoutsaris, S., Zahn, M. and Berrisford, P. (2013) The changing energy balance of the polar regions in a warmer climate. *Journal of Climate*, 26, 3112–3129.
- Boisvert, L.N. and Stroeve, J.C. (2015) The Arctic is becoming warmer and wetter as revealed by the atmospheric infrared sounder. *Geophysical Research Letters*, 42, 4439–4446.
- Cohen, L., Hudson, S.R., Walden, V.P., Graham, R.M. and Granskog, M.A. (2017) Meteorological conditions in a thinner Arctic sea ice regime from winter to summer during the Norwegian Young Sea Ice expedition (N-ICE2015). *Journal of Geophysical Research: Atmospheres*, 122, 7235–7259.
- Dahlke, S. and Maturilli, M. (2017) Contribution of atmospheric advection to the amplified winter warming in the Arctic North Atlantic region. *Advances in Meteorology*, 2017, 4928620. <https://doi.org/10.1155/2017/4928620>.
- Dee, D.P., Uppala, S.M., Simmons, A.J., Berrisford, P., Poli, P., Kobayashi, S., Andrae, U., Balmaseda, M.A., Balsamo, G., Bauer, P., Bechtold, P., Beljaars, A.C.M., van de Berg, L., Bidlot, J., Bormann, N., Delsol, C., Dragani, R., Fuentes, M., Geer, A.J., Haimberger, L., Healy, S.B., Hersbach, H., Hólm, E.V., Isaksen, I., Kållberg, P., Köhler, M., Matricardi, M., McNally, A.P., Monge-Sanz, B.M., Morcrette, J.J., Park, B.-K., Peubey, C., De Rosnay, P., Tavolato, C., Thépaut, J.-N. and Vitart, F. (2011) The ERA-Interim reanalysis: configuration and performance of the data assimilation system. *Quarterly Journal of the Royal Meteorological Society*, 137(656), 553–597.
- Ding, Q.H., Schweiger, A., L'Heureux, M., Battisti, D.S., Po-Chedley, S., Johnson, N.C., Blanchard-Wrigglesworth, E., Harnos, K., Zhang, Q., Eastman, R. and Steig, E.J. (2017) Influence of high-latitude atmospheric circulation changes on summertime Arctic sea ice. *Nature Climate Change*, 7, 289–295.
- Dufour, A., Zolina, O. and Gulev, S.K. (2016) Atmospheric moisture transport to the Arctic: assessment of reanalyses and analysis of transport components. *Journal of Climate*, 29, 5061–5081.
- Gong, T.T., Feldstein, S. and Lee, S. (2017) The role of downward infrared radiation in the recent Arctic winter warming trend. *Journal of Climate*, 30, 4937–4949.

- Graham, R.M., Cohen, L., Petty, A.A., Boisvert, L.N., Rinke, A., Hudson, S.R., Nicolaus, M. and Granskog, M.A. (2017a) Increasing frequency and duration of Arctic winter warming events. *Geophysical Research Letters*, 44, 6974–6983.
- Graham, R.M., Rinke, A., Cohen, L., Hudson, S.R., Walden, V.P., Granskog, M.A., Dorn, W., Kayser, M. and Maturilli, M. (2017b) A comparison of the two Arctic atmospheric winter states observed during N-ICE2015 and SHEBA. *Journal of Geophysical Research: Atmospheres*, 122, 5716–5737.
- Graversen, R.G. (2006) Do changes in the midlatitude circulation have any impact on the Arctic surface air temperature trend? *Journal of Climate*, 19, 5422–5438.
- Graversen, R.G. and Burtu, M. (2016) Arctic amplification enhanced by latent energy transport of atmospheric planetary waves. *Quarterly Journal of the Royal Meteorological Society*, 142(698), 2046–2054.
- Graversen, R.G. and Langen, P.L. (2019) On the role of the atmospheric energy transport in $2 \times \text{CO}_2$ -induced polar amplification in CESM1. *Journal of Climate*, 32, 3941–3956.
- Graversen, R.G., Mauritsen, T., Tjernström, M., Källén, E. and Svensson, G. (2008) Vertical structure of recent Arctic warming. *Nature*, 451, 53–56.
- Heiskanen, T., Graversen, R.G., Rydsaa, J.H. and Isachsen, P.E. (2020) Comparing wavelet and Fourier perspectives on the decomposition of meridional energy transport into synoptic and planetary components. *Quarterly Journal of the Royal Meteorological Society*, 146(731), 2717–2730.
- Hersbach, H., Bell, B., Berrisford, P., Hirahara, S., Horányi, A., Muñoz-Sabater, J., Nicolas, J., Peubey, C., Radu, R., Schepers, D., Simmons, A., Soci, C., Abdalla, S., Abellan, X., Balsamo, G., Bechtold, P., Biavati, G., Bidlot, J., Bonavita, M., De Chiara, G., Dahlgren, P., Dee, D.P., Diamantakis, M., Dragani, R., Flemming, J., Forbes, R., Fuentes, M., Geer, A., Haimberger, L., Healy, S., Hogan, R.J., Hólm, E., Janisková, M., Keeley, S., Laloyaux, P., Lopez, P., Lupu, C., Radnoti, G., de Rosnay, P., Rozum, I., Vamborg, F., Villaume, S. and Thépaut, J.-N. (2020) The ERA5 global reanalysis. *Quarterly Journal of the Royal Meteorological Society*, 146(730), 1999–2049.
- Hodges, K.I. (1999) Adaptive constraints for feature tracking. *Monthly Weather Review*, 127, 1362–1373.
- Holton, J.R. and Hakim, G.J. (2013) An introduction to dynamic meteorology. 5 ed. Vol. 88, 552 pp.
- Hwang, Y.-T., Frierson, D.M.W. and Kay, J.E. (2011) Coupling between Arctic feedbacks and changes in poleward energy transport. *Geophysical Research Letters*, 38(17). <https://doi.org/10.1029/2011GL048546>.
- Inoue, J., Hori, M.E. and Takaya, K. (2012) The role of Barents Sea ice in the wintertime cyclone track and emergence of a warm-Arctic cold-Siberian anomaly. *Journal of Climate*, 25, 2561–2568.
- Koenigk, T., Brodeau, L., Graversen, R.G., Karlsson, J., Svensson, G., Tjernström, M., Willén, U. and Wyser, K. (2013) Arctic climate change in 21st century CMIP5 simulations with EC-Earth. *Climate Dynamics*, 40, 2719–2743.
- Liu, C.J. and Barnes, E.A. (2015) Extreme moisture transport into the Arctic linked to Rossby wave breaking. *Journal of Geophysical Research: Atmospheres*, 120, 3774–3788.
- Papritz, L. and Dunn-Sigouin, E. (2020) What configuration of the atmospheric circulation drives extreme net and total moisture transport into the Arctic. *Geophysical Research Letters*, 47(17), e2020GL089769.
- Park, D.S.R., Lee, S. and Feldstein, S.B. (2015) Attribution of the recent winter sea ice decline over the Atlantic sector of the Arctic Ocean. *Journal of Climate*, 28, 4027–4033.
- Peixoto, J.P. and Oort, A.H. (1992) *Physics of Climate*. New York, NY: American Institute of Physics.
- Rinke, A., Maturilli, M., Graham, R.M., Matthes, H., Handorf, D., Cohen, L., Hudson, S.R. and Moore, J.C. (2017) Extreme cyclone events in the Arctic: wintertime variability and trends. *Environmental Research Letters*, 12, 094006.
- Serreze, M.C. and Barry, R.G. (2011) Processes and impacts of Arctic amplification: a research synthesis. *Global and Planetary Change*, 77, 85–96.
- Serreze, M.C. and Francis, J.A. (2006) The Arctic amplification debate. *Climatic Change*, 76, 241–264.
- Simmonds, I., Burke, C. and Keay, K. (2008) Arctic climate change as manifest in cyclone behavior. *Journal of Climate*, 21, 5777–5796.
- Skific, N. and Francis, J.A. (2013) Drivers of projected change in Arctic moist static energy transport. *Journal of Geophysical Research: Atmospheres*, 118, 2748–2761.
- Trenberth, K.E. (1991) Climate diagnostics from global analyses: conservation of mass in ECMWF analyses. *Journal of Climate*, 4, 707–722.
- Woods, C. and Caballero, R. (2016) The role of moist intrusions in winter Arctic warming and sea ice decline. *Journal of Climate*, 29, 4473–4485.
- Woods, C., Caballero, R. and Svensson, G. (2013) Large-scale circulation associated with moisture intrusions into the Arctic during winter. *Geophysical Research Letters*, 40, 4717–4721.
- Yoshimori, M., Abe-Ouchi, A. and Laine, A. (2017) The role of atmospheric heat transport and regional feedbacks in the Arctic warming at equilibrium. *Climate Dynamics*, 49, 3457–3472.

SUPPORTING INFORMATION

Additional supporting information may be found online in the Supporting Information section at the end of this article.

How to cite this article: Rydsaa JH, Graversen RG, Heiskanen TIH, Stoll PJ. Changes in atmospheric latent energy transport into the Arctic: Planetary versus synoptic scales. *QJR Meteorol Soc.* 2021;147:2281–2292. <https://doi.org/10.1002/qj.4022>